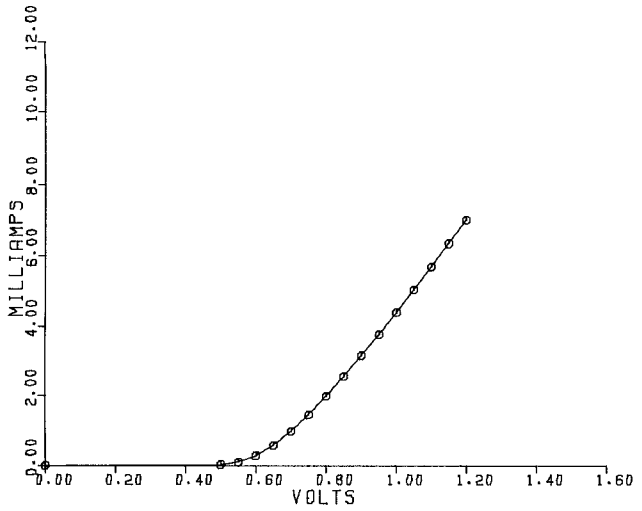

Fig. 4. $I-V$ characteristic of Schottky diode

IV. Conclusions

Models for lossy transmission lines and Schottky diodes have been installed into SPICE 2G.6. The models offer capabilities not previously available in the public domain. Although these models can (and have been) implemented into SPICE as subcircuit models, our installation directly into the source code of SPICE yields execution times typically five times faster, according to numerical experiments performed by us.

Interested readers should contact the authors concerning arrangements for distributing the modified SPICE source code (which also includes our previous released models for enhancement- and depletion-mode GaAs FET's [2]). It should be noted that the models described here are not directly compatible with SPICE 3A7. One reason for this is that version 3A7 is written in the C programming language, while SPICE 2G.6 is written in Fortran.

Appendix I
User's Guide for the Lossy Transmission Line Model

Model Usage:

Txxx n1 n2 n3 n4 param1 = val1, param2 = val2, ..., Skin

Notes:

n1 n2: Nodes at port 1 of the transmission line

n3 n4: Nodes at port 2

Skin: If this word is present, then skin effect calculations are performed.

Example:

T1 1 0 2 0 Z0 = 50 Td = 1ns NL = 1 NorLc = 10 Nr = 10 Skin

Parameter Variable	*Parameter Description*	*Default Value*
Z0 (a Z and a zero)	Characteristic impedance (ohms)	—
Td	Transmission delay (seconds)	—
NL	Electrical length of Line in number of wavelengths	0.25
F	Frequency at which line is NL wavelengths long (Hz)	—
Nr	Resistance per unit wavelength of line (ohms/wavelength)	0.0
NorLc	Number of elemental sections used within SPICE to model lossy line	10

Note. 1 At most 2 of the parameters Td, NL, and F should be specified since the relation Td = NL/F is enforced in SPICE.

2 NorLc need be specified only if Nr is not equal to zero.

Appendix II
User's Guide for the Schottky Diode

Model Usage:

Dxxx n1 n2 Your_Model_Name

.Model Your_Model_Name Sd(param1 = val1, param2 = val2, ...)

Notes:

n1: Anode

n2: Cathode

Example:

D1 2 0 Schottky

.Model Schottky Sd(Is = 0.3p Rs = 70.0 N = 1.05 Rss = 90 Iss = 14.4u Ns = 0.389)

Parameter Variable	*Parameter Description*	*Default Value*
Is	Saturation current for principal diode (D1 in Fig. 3)	1e-14
Iss	Saturation current for auxiliary diode (D2 in Fig. 3)	1e-14
Rs	Ohmic + bulk resistance of principal diode	0.0
Rss	Schottky spreading resistance	36.0
N	Emission coefficient of principal diode	1.0
Ns	Emission coefficient of auxiliary diode	1.0

References

[1] L. W. Nagel, "SPICE2: A computer program to simulate semiconductor circuits," Electron. Res. Lab., Univ. California, Berkeley, Memo ERL-M520, 1975

[2] S. E. Sussman-Fort, J. C. Hantgan, and F. L. Huang, "A SPICE model for enhancement and depletion mode GaAs FETs," *IEEE Trans. Microwave Theory Tech.*, vol. MTT-34, pp. 1115–1119, Nov. 1986

[3] S. E. Sussman-Fort, "A complete GaAs MESFET computer model for SPICE," *IEEE Trans. Microwave Theory Tech.*, vol. MTT-32, pp. 471–473, Apr. 1984

[4] S. E. Sussman-Fort and J. C. Hantgan, "A SPICE installed model for enhancement and depletion mode GaAs FETs," in *Proc. Int. Symp. Circuits Syst.* (Philadelphia, PA), May 4–7, 1987 (invited paper)

[5] A. J. Gruodis, "Transient analysis of uniform resistive transmission lines in a homogeneous medium," *IBM J. Res. Develop.*, vol. 23, no. 6, pp. 675–681, Nov. 1979.

[6] C. S. Yen *et al.*, "Time domain skin-effect model analysis of lossy transmission lines," *Proc. IEEE*, vol. 70, pp. 750–757, July 1982.

[7] F. H. Branin, Jr., "Transient analysis of lossless transmission lines," *Proc. IEEE*, vol. 55, p. 2012, 1967.

[8] H. W. Dommel, "Digital computer simulation of electromagnetic transients in single and multiphase networks," *IEEE Trans. Power App. Syst.*, vol. PAS-88, p. 388, 1969.

[9] P. A. Brennan and A. E. Ruehli, "Time-domain skin-effect model using resistors and lossless transmission lines," *IBM Technical Disclosure Bulletin*, vol. 21, no. 5, pp. 2162–2163, Oct. 1978

[10] R. S. Pengelly, *Microwave Field-Effect Transistors—Theory, Design and Applications*. Chichester, England: Wiley, 1982, p. 161

[11] D. B. Estreich, "A simulation model for Schottky diodes in GaAs integrated circuits," *IEEE Trans. Computer-Aided Design*, vol. CAD-2, no. 2, pp. 106–111, Apr. 1983

Propagation Losses in Dielectric Image Guides

JIQING XIA, STEPHEN W. MCKNIGHT, AND CARMINE VITTORIA

***Abstract*—To evaluate low-loss transmission lines for integrated circuits operating at millimeter wavelengths, we have calculated the propagation**

Manuscript received May 22, 1987; revised August 25, 1987. This work was supported in part by the ONR under Contract N00014-86-K-0534.

The authors are with the Center for Electromagnetics Research, Electrical and Computer Engineering Department, Northeastern University, Boston, MA 02115

IEEE Log Number 8717594.

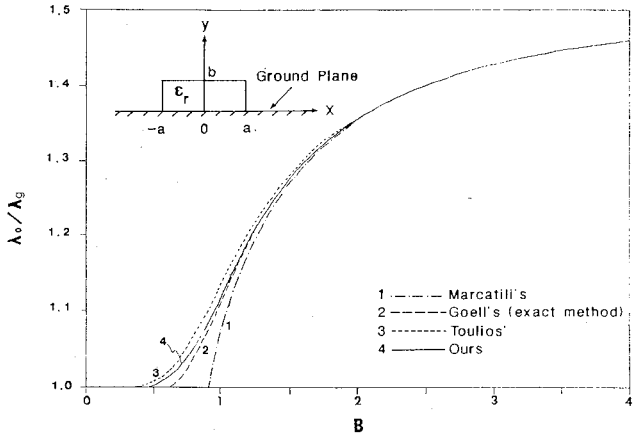

Fig. 1. Image guide wavelength λ_g plotted as a function of normalized dimension parameter B, where $B=(4b/\lambda_0)[\mathrm{Re}(\epsilon_r)-1]^{1/2}$, $\epsilon_r=2.25$, and $a/b=1$. Upper left: cross sectional view of dielectric image guide.

losses of a dielectric image guide using the effective dielectric constant (EDC) method to a higher order of approximation than previously reported work. Our results differ significantly from other EDC calculations close to the waveguide cutoff frequency. In this region, we find that there is a minimum in the waveguide attenuation that has not been alluded to in the literature, and also a peak in the imaginary parts of the transverse propagation constants related to dimensional resonances within the waveguide. These results imply that the propagation losses will be lowered and the fields will be more effectively confined within the waveguide at frequencies close to the cutoff. Thus, it may be advantageous when using dielectric image guides for low-loss transmission line applications to operate near cutoff where the corrections included in our calculations are critical.

I. Introduction

The image guide is a simple waveguide structure used often for millimeter-wave integrated circuits, as shown in Fig. 1. Marcatili [1] calculated approximately the propagation characteristics of the dielectric image guide. Toulios and Knox [3] followed Marcatili's approximate method and introduced an effective dielectric constant (EDC) method of calculation. It is the most commonly used method for calculating the propagation characteristics of dielectric waveguides [4]–[7]. More accurate solutions were obtained by Goell [2] using infinite mode solution technique. Other calculations used the mode-matching technique [8]–[10], the generalized telegraphers' equations [11], or the finite element iterative method [12]. All these methods involve considerably more computational complexity than the EDC method.

In this paper, we have calculated the dispersion and dielectric and conductivity losses as a function of frequency. We have adopted the EDC method but included in our calculations an additional factor which was ignored in previous calculations [1], [3]. This factor arises simply from proper application of Maxwell's equations to this problem. Using this factor in the transcendental equation for transverse propagation constant allows us to obtain improved results which show significant differences from previous work.

II. Method of Analysis

Our analysis shares several basic assumptions with the previous [1], [3] approximate methods. These are the single-mode assumption, field distribution assumption, and large-aspect-ratio assumption. All these assumptions were described in the literature [4], [5].

In Fig. 1, for the E_{11}^y mode, the field components in terms of H_x are

$$H_y = 0 \tag{1a}$$

$$H_z = -\frac{j}{k_z}\frac{\partial h_x}{\partial x} \tag{1b}$$

$$E_x = -\frac{1}{\omega\epsilon k_z}\frac{\partial^2 h_x}{\partial y \partial x} \tag{1c}$$

$$E_y = \frac{1}{\omega\epsilon k_z}\left(k_y^2 - k^2\right)h_x \tag{1d}$$

$$E_z = \frac{j}{\omega\epsilon}\frac{\partial h_x}{\partial y} \tag{1e}$$

where ϵ is the dielectric constant, $\omega = 2\pi f$, f is the frequency, k_x, k_y, and k_z are propagation constants in the dielectric, and

$$k^2 = \omega^2\mu_0\epsilon \qquad k_0^2 = \omega^2\mu_0\epsilon_0 = \left(\frac{2\pi}{\lambda_0}\right)$$

and λ_0 is the free-space wavelength.

Applying (1) to boundary conditions as in previous calculations [1], [3], we obtained the following equations for the transverse propagation constant k_x:

$$k_x a = \frac{m\pi}{2} - \tan^{-1}\left(\frac{k_x}{k_{x0}}\cdot\frac{F_0}{F_1}\right), \qquad m = 1,2,3,\cdots \tag{2}$$

where

$$k_{x0} = \left[(\epsilon_{re}-1)k_0^2 - k_x^2\right]^{1/2} \tag{3}$$

$$\epsilon_{re} = \epsilon_r - \left(\frac{k_y}{k_0}\right)^2 \tag{4}$$

$$F_0 = 1 - \frac{k_y^2}{k_0^2} \qquad F_1 = 1 - \left(\frac{k_y^2}{\epsilon_r k_0^2}\right). \tag{5}$$

Previous authors [1], [3] approximate the factor $(k_y^2 - k^2)$ in (1d) as $(-k^2)$, omitting the k_y^2 term. At high frequencies, $k_0^2 \gg k_y^2$ so that $F_0/F_1 = 1$, which gives exactly Toulios's or Marcatili's expression for k_x. Hence, at high frequencies, their approximation is quite reasonable. At low frequencies, $k_y^2 \sim k_0^2$ so that $F_0/F_1 \neq 1$, and their approximation [1], [3] may not be appropriate.

To allow for small losses in the dielectric rod, a complex dielectric constant is introduced, $\epsilon' - j\epsilon''$. This means that the propagation constants k_x, k_y, and k_z are also complex.

The guide wavelength is defined as

$$\lambda_g = \frac{2\pi}{\mathrm{Re}(k_z)}. \tag{6}$$

As in previous publication λ_g is normalized with respect to the free-space wavelength so that λ_0/λ_g is plotted as a function of a normalized dimension,

$$B = \frac{4b}{\lambda_0}\sqrt{\mathrm{Re}(\epsilon_r) - 1}. \tag{7}$$

In a similar manner the dielectric propagation losses are normalized with respect to an infinite medium propagation loss, α_∞, or

$$\alpha_D = \frac{\alpha_\epsilon}{\alpha_\infty}$$

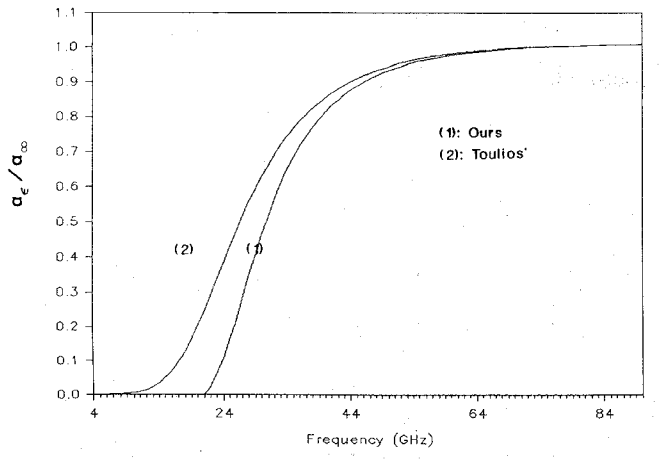

Fig. 2. Dielectric propagation losses are plotted as a function of frequency for the fundamental E_{11}^y mode of propagation ($\epsilon_r = 2 - j3\times10^{-4}$, $a = b = 0.25$ cm).

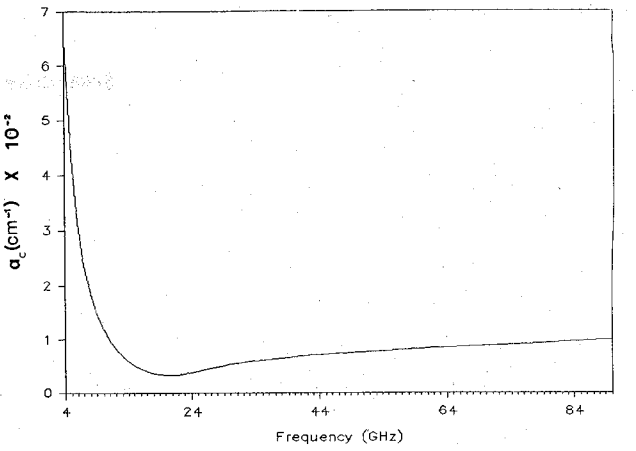

Fig. 3. Conductivity propagation losses are plotted as a function of frequency for the fundamental E_{11}^y mode of propagation ($\epsilon_r = 2 - j3\times10^{-4}$, $a = b = 0.25$ cm).

where

$$\alpha_\epsilon = -\mathrm{Im}(k_z) \tag{8}$$

$$\alpha_\infty = \frac{\pi\sqrt{\mathrm{Re}(\epsilon_r)}}{\lambda_0}\tan\delta \tag{9}$$

and

$$\tan\delta = \frac{\epsilon''}{\epsilon'}.$$

The attenuation constant α_c due to conductor losses can be calculated from

$$\alpha_c = \frac{W_L}{2W_T} \tag{10}$$

where W_L is the power lost per unit length and W_T is the total power transmitted (including power outside of guide). The integral expressions for W_L and W_T are contained in [3].

The total propagation loss, due to both dielectric and conductor losses for the image guide, is given by

$$\alpha_{\text{total}} = \alpha_\epsilon + \alpha_c. \tag{11}$$

III. Calculations and Results

Solving the transcendental equation (2), we have calculated dispersion, dielectric losses, and conductor losses of a dielectric image guide as shown in Fig. 1. For comparison purpose, we have also used Marcatili's [1] and Toulios's [3] approximations. In addition, we have compared the dispersions obtained with the exact method of Goell [2]. The comparison between our results of dispersion and the others is shown in Fig. 1. Our curve is closer to the exact curve of Goell's [2] than either of the other approximate methods. At high frequencies, all the curves overlap each other. This is understandable, since $k_y^2 \ll k_0^2$.

The dielectric and conductivity loss curves are plotted in Figs. 2 and 3, respectively. In Fig. 2, the dielectric loss in our calculation approaches zero much faster than that in Toulios's results at low frequencies. In our curve, the dielectric propagation losses approach zero at 22 GHz, while in Toulios's there are significant losses until 8 GHz. Both calculation methods predict the same results for frequencies above 55 GHz.

In Fig. 3 we show the conductivity losses calculated as a function of frequency. At frequencies lower than 10 GHz, the conductivity losses in our calculation are much higher than those predicted by Toulios. At high frequencies, the two methods again are in very good agreement. We note that there is a minimum in the conductivity losses near the cutoff of the image guide. This minimum was not previously noted in the literature.

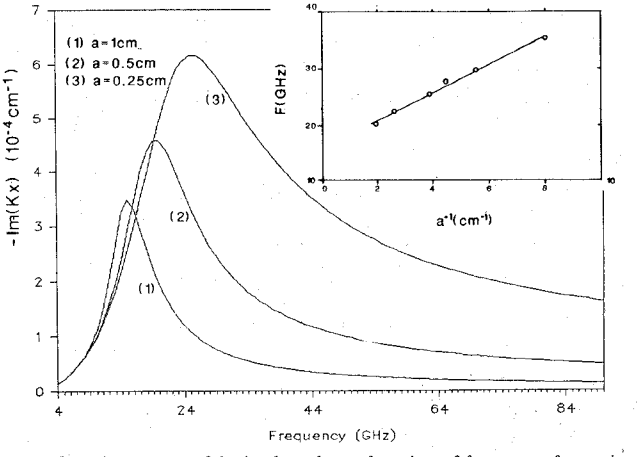

Fig. 4. Imaginary part of k_x is plotted as a function of frequency for various values of a. Upper right: resonant frequency of $\mathrm{Im}(k_x)$ is plotted as a function of a^{-1}.

We have plotted the imaginary part of the transverse wave vector k_x as a function of frequency in Fig. 4. We see that there is a maximum in $|\mathrm{Im}(k_x)|$ at low frequencies. We find a typical resonant behavior with a resonance frequency of 25 GHz for the square-cross-section guide considered above (curve 3). A similar peak is obtained in $|\mathrm{Im}(k_y)|$ at slightly lower frequency. Near these maxima the fields are more effectively confined within the waveguide.

In order to establish the cause of these peaks, we calculated the imaginary parts of k_x and k_y for various values a and b, which are the cross dimensions of the image guide. As shown in the inset of Fig. 4, the peak frequency of $|\mathrm{Im}(k_x)|$ is inversely proportional to a. In fact, if we plot the frequency of the peak of either $-\mathrm{Im}(k_x)$ or $-\mathrm{Im}(k_y)$ as a function of a^{-1} or b^{-1}, respectively, we find approximately linear relationships, as shown in Fig. 4 for k_x. Thus, we conclude the resonant behavior in the losses is related to geometrical factors—very similar to the so-called dielectric resonance behavior in materials of the finite dimension.

Our results suggest that the attenuation of the waveguide is significantly lower near cutoff than at high frequencies and that the dimensional resonance can be utilized at the same frequency to more effectively confine the wave to within the dielectric. This implies that operation of a dielectric image guide near cutoff may be advantageous for some purposes. Near cutoff the dispersion and attenuation are strong functions of the frequency; therefore our more exact approximate calculation may be critical for the design of devices in this region.

IV. Discussions and Conclusions

We introduced a new factor F_0/F_1 (which arises simply from Maxwell's equations) into the transcendental equation for the transverse propagation constant. Using this higher order approximate equation, we have calculated dispersion, dielectric losses, and conductivity losses of a dielectric image guide. Our results differ significantly from previous results [3] at low frequencies. We found that propagation losses have a minimum at low frequencies near cutoff. In addition, we found that the transverse attenuations show resonance behavior. Such resonances are dimensionally related. By measuring coupling losses near cutoff, it may be possible to characterize precisely the mode characteristics of an image guide. Our new results suggest that the operation of a dielectric image guide near cutoff may be advantageous for some applications.

Acknowledgment

The authors wish to express appreciation to J. Diaz for his discussion and aid in programming.

References

[1] E. A. J. Marcatili, "Dielectric rectangular waveguide and direction coupler for integrated optics," *Bell Syst. Tech. J.*, vol. 48, no. 7, pp. 2079–2102, Sept. 1969.

[2] J. E. Geoll, "A circular-harmonic computer analysis of rectangular dielectric waveguides," *Bell Syst. Tech. J.*, vol. 48, no. 7, pp. 2133–2160, Sept. 1969.

[3] P. P. Toulios and R. M. Knox, "Rectangular dielectric image lines for millimeter integrated circuits," in *Proc. Wescon Conf.* (Los Angeles, CA), 1970, pp. 1–10.

[4] R. M. Knox and P. Toulios, "Integrated circuits for the millimeter through optical frequency range," in *Proc. Symp. Submillimeter Waves* (NY), Apr. 1–2, 1970, pp. 497–516.

[5] W. McLevige, T. Itoh and R. Mittra, "New waveguide structures for millimeter wave and optical integrated circuits," *IEEE Trans. Microwave Theory Tech.*, vol. MTT-23, pp. 788–794, Oct. 1975.

[6] P. Bhartia and I. J. Bahl, *Millimeter Wave Engineering and Applications*. New York: Wiley, 1984, ch. 6.

[7] T. Itoh, "Inverted strip dielectric waveguide for millimeter-wave integrated circuits," *IEEE Trans. Microwave Theory Tech.*, vol. MTT-24, pp. 821–827, Nov. 1976.

[8] K. Solbach and I. Wolff, "The electromagnetic fields and phase constants of dielectric image lines," *IEEE Trans. Microwave Theory Tech.*, vol. MTT-26, pp. 266–274, Apr. 1978.

[9] R. Mittra, Y. L. Hou, and V. Jamnejad, "Analysis of open dielectric waveguides using mode matching technique and variational methods," *IEEE Trans. Microwave Theory Tech.*, vol. MTT-28, pp. 36–43, Jan. 1980.

[10] U. Crombach, "Analysis of single and coupled rectangular dielectric waveguides," *IEEE Trans. Microwave Theory Tech.*, vol. MTT-29, pp. 870–874, Sept. 1981.

[11] K. Oguso, "Numerical analysis of the rectangular dielectric waveguide and its modifications," *IEEE Trans. Microwave Theory Tech.*, vol. MTT-25, pp. 874–885, Nov. 1977.

[12] M. Ikeuchi, H. Sawami, and H. Niki, "Analysis of open-type dielectric waveguides by the finite element iterative method," *IEEE Trans. Microwave Theory Tech.*, vol. MTT-29, pp. 234–239, Mar. 1981.

A 4.5-GHz GaAs Dual-Modulus Prescaler IC

MASANOBU OHHATA, MEMBER, IEEE, TOHRU TAKADA, MASAYUKI INO, MEMBER, IEEE, NAOKI KATO, MEMBER, IEEE, AND MASAO IDA

***Abstract*—A 4.5-GHz 100-mW GaAs divide-by-256/258 dual-modulus prescaler with a reset function has been developed. The operating frequency obtained for this modulus prescaler is the highest to date, while the power dissipation is comparable to others that have been reported. The supply voltage is as low as 3 V. A low-power, source coupled FET logic (LSCFL) using novel level shift circuits and 0.5-μm-gate buried P-layer SAINT (BP-SAINT) FET's have been used to achieve this high performance.**

I. Introduction

Prescaler IC's that operate in the gigahertz frequency range under low power dissipation are required for battery-operated portable radios. Many prescalar IC's using low power, source coupled FET logic (LSCFL) [1] have been fabricated to take advantage of the excellent characteristics of this logic, such as high speed and large noise margin. Several attempts to reduce the operating current at a 4 to 5 V supply voltage have been reported [2], [3].

In this letter, we report an even lower supply voltage operation. Not only by reducing the current, but also lowering the supply voltage is an effective way to extend the battery lifetime by changing the battery connection to parallel. Alternatively, by lowering the supply voltage, fewer batteries are needed. This can obviously help to reduce radio size and weight.

A 4.5-GHz 100-mW GaAs divide-by-256/258 dual-modulus prescaler with a reset function has been successfully fabricated using a three-level series gate LSCFL with novel level shift circuits [4] and new FET fabrication technology (buried P-layer SAINT) [5]. The 4.5-GHz operation is the highest modulus prescalar so far reported. The supply voltage, at 3 V, is the lowest value reported among LSCFL prescaler IC's. In addition, a reset function has been introduced to the newly designed prescaler for a phase-initialized frequency synthesizer [6] to reduce standby power dissipation.

II. Circuit Design

A block diagram of the fabricated divide-by-256/258 dual-modulus prescaler is shown in Fig. 1. The prescaler consists of three D-type master–slave flip-flops (D-FF's), six T-type master–slave flip-flops (T-FF's), two NOR gates, three OR gates, and four I/O buffers. These circuits are constructed using a three-level series gate LSCFL that offers the advantages of high speed, low power dissipation, and wide allowable threshold voltage variation, because of its true and complementary operation [1]. The NOR1 and NOR2 gates are included in DFF1 and DFF3, respectively, using a series gating technique. All FET's are normally-off types with a threshold voltage of 0.1 V. Divide-by-256 and 258 operations are selected by a mode control terminal (MC). Divide-by-256 is selected when the MC is set at a high level, and divide-258 is selected when the MC is set at a low level, or left open. The output signal is fixed at the low level when the reset terminal (R) is set at the high level. This reset function is the first attempt for the phase-initialized frequency synthesizer.

Manuscript received March 16, 1987; revised August 14, 1987.

The authors are with the NTT Electrical Communications Laboratories, Atsugi-shi, Kanagawa Prefecture, 243-01, Japan.

IEEE Log Number 8717593